Chemical Engineering Journal 296 (2016) 406–411

Contents lists available at ScienceDirect

Chemical Engineering Journal

journal homepage: www.elsevier.com/locate/cej

Short communication

Improving hydrogen yields, and hydrogen:steam ratio in the chemical looping production of hydrogen using $Ca_2Fe_2O_5$

Martin S.C. Chan [a,*], Wen Liu [b], Mohammad Ismail [c], Yanhui Yang [b,d], Stuart A. Scott [c], John S. Dennis [a]

[a] Department of Chemical Engineering and Biotechnology, University of Cambridge, CB2 3RA, United Kingdom
[b] Cambridge Centre for Advanced Research in Energy Efficiency in Singapore, Nanyang Technological University, Singapore 138602, Singapore
[c] Department of Engineering, University of Cambridge, CB2 1PZ, United Kingdom
[d] School of Chemical and Biomedical Engineering, Nanyang Technological University, Singapore 637459, Singapore

HIGHLIGHTS

- Mixed oxides of iron and calcium were examined as oxygen carriers.
- Thermodynamic improvements in the yield of hydrogen were obtained, as predicted.
- The oxidising potential of oxygen carrier materials is important in their design.
- Modifications of reactors that exploit this improved property are proposed.

ARTICLE INFO

Article history:
Received 26 January 2016
Received in revised form 22 March 2016
Accepted 26 March 2016
Available online 1 April 2016

Keywords:
Chemical looping
Hydrogen
Iron oxide
Thermodynamics
Packed bed

ABSTRACT

A thermodynamic property of $Ca_2Fe_2O_5$ was exploited to improve the efficiency of the steam-iron process to produce hydrogen. The ability of reduced $Ca_2Fe_2O_5$ to convert a higher fraction of steam to hydrogen than chemically unmodified Fe was demonstrated in a packed bed. At 1123 K, the use of $Ca_2Fe_2O_5$ achieved an equilibrium conversion of steam to hydrogen of 75%, in agreement with predicted thermodynamics and substantially higher than that theoretically achievable by iron oxide, *viz.* 62%. Furthermore, in $Ca_2Fe_2O_5$, the full oxidation from Fe(0) to Fe(III) can be utilised for hydrogen production – an improvement from the Fe to Fe_3O_4 transition for unmodified iron. Thermodynamic considerations demonstrated in this study allow for the rational design of oxygen carriers in the future. Modifications of reactors to capitalise on this new material are discussed.

1. Introduction

The use of hydrogen as an energy vector is dependent on efficiently minimising the carbon emissions associated with its production [1]. Steam-reforming of methane is currently the dominant source of hydrogen but it is energy intensive and requires operation at large scale to be economic [2,3]. A proposed alternative to steam reforming is to use the chemical looping of iron oxide to produce H_2, otherwise known as the steam-iron process. Use of looping reactions for this purpose dates back to the late 19th and early 20th Century [4]. This process is summarised in the following scheme:

(I) Successive reduction of the oxide by synthesis gas (or some hydrocarbon fuel) to produce CO_2 and H_2O (where z and z' refer to the non-stoichiometry of the wüstite phase (Fe_zO), and enthalpies of reaction correspond to $z = 0.947$ where appropriate):

$$3Fe_2O_{3(s)} + CO_{(g)} \rightleftharpoons 2Fe_3O_{4(s)} + CO_{2(g)} \quad \Delta H^{\circ}_{1123\,K} = -38.1\ kJ\ mol^{-1} \tag{1}$$

$$\frac{z}{4z-3}Fe_3O_{4(s)} + CO_{(g)} \rightleftharpoons \frac{3}{4z-3}Fe_zO_{(s)} + CO_{2(g)} \quad \Delta H^{\circ}_{1123\,K} = +21.1\ kJ\ mol^{-1} \tag{2}$$

$$Fe_{z'}O_{(s)} + CO_{(g)} \rightleftharpoons \frac{1}{z'}Fe_{(s)} + CO_{2(g)} \quad \Delta H^{\circ}_{1123\,K} = -16.7\ kJ\ mol^{-1} \tag{3}$$

* Corresponding author.
E-mail address: mscc3@cam.ac.uk (M.S.C. Chan).

http://dx.doi.org/10.1016/j.cej.2016.03.132
1385-8947/

$$3Fe_2O_{3(s)} + H_{2(g)} \rightleftharpoons 2Fe_3O_{4(s)} + H_2O_{(g)} \quad \Delta H^\circ_{1123\,K} = -4.5\ kJ\ mol^{-1} \tag{4}$$

$$\frac{z}{4z-3}Fe_3O_{4(s)} + H_{2(g)} \rightleftharpoons \frac{3}{4z-3}Fe_zO_{(s)} + H_2O_{(g)}$$
$$\Delta H^\circ_{1123\,K} = +54.6\ kJ\ mol^{-1} \tag{5}$$

$$Fe_{z'}O_{(s)} + H_{2(g)} \rightleftharpoons \frac{1}{z'}Fe_{(s)} + H_2O_{(g)} \quad \Delta H^\circ_{1123\,K} = +16.8\ kJ\ mol^{-1} \tag{6}$$

(II) Oxidation of the reduced solid by H_2O to produce H_2 (reverse of reactions 5 and 6).

(III) Oxidation of the magnetite (Fe_3O_4) by air to generate heat and remove any carbonaceous deposits:

$$2Fe_3O_{4(s)} + 0.5O_{2(g)} \rightleftharpoons 3Fe_2O_{3(s)} + \quad \Delta H^\circ_{1123\,K} = -244.1\ kJ\ mol^{-1} \tag{7}$$

This approach offers the advantages of (i) achieving an inherent separation of CO_2 if conducted in a packed bed reactor, (ii) being potentially thermally neutral, and (iii) the economics being less dependent on the scale of the process. As a consequence of (iii), a process based on chemical looping would be suited to the local production of H_2 from any gasified fuel. The advantages of a packed bed reactor configuration have been described previously by Bohn *et al.* [5].

An important variable affecting the efficiency of the process is the conversion of steam to hydrogen by the reverse of reactions 5 and 6 in stage (II). Low conversions of steam requires additional steam to be generated or recycled, both of which require additional inputs of energy [6]. Using unmodified iron oxide, the maximum conversion of the steam is limited by the thermodynamic equilibria of reactions 5 and 6, with equilibrium constants K_{p5} and K_{p6}, which also represent the oxidising potentials of the phase transitions in terms of partial pressures pO_2, pH_2O/pH_2, or pCO_2/pCO. For example at 1123 K, the conversion of steam to hydrogen by metallic iron and wüstite (Fe_zO) is thermodynamically limited to 62% and 21%, respectively (calculated from data obtained by Giddings and Gordon [7]). However, the formation of a ternary oxide phase, by mixing iron with other elements, could, potentially, enhance the stability of Fe(II) and Fe(III) under reducing environments, lowering the oxidising potentials of the transition from metallic Fe to Fe(II) and Fe(III) and hence increasing the conversion of steam. Previous work on mixed oxides with the potential to improve steam conversion in the thermodynamic limit for the production of hydrogen include the Ca-Fe-O system [8] and the perovskite $La_{0.8}Sr_{0.2}FeO_{3-\delta}$ (LSF) [9].

This paper focuses on $Ca_2Fe_2O_5$, a phase recently studied for its potential in chemical looping [8]. It undergoes a single phase transition from Fe^{3+} to Fe^0 in

$$2CaO_{(s)} + 2Fe_{(s)} + 3H_2O_{(g)} \rightleftharpoons Ca_2Fe_2O_{5(s)} + 3H_{2(g)}$$
$$\Delta H^\circ_{1123\,K} = -107.9\ kJ\ mol^{-1} \tag{8}$$

$$Ca_2Fe_2O_{5(s)} + 3CO_{(g)} \rightleftharpoons 2CaO_{(s)} + 2Fe_{(s)} + 3CO_{2(g)}$$
$$\Delta H^\circ_{1123\,K} = +7.05\ kJ\ mol^{-1} \tag{9}$$

where enthalpies have been calculated from the results of Jacob *et al.* [10] (verified with MTData using the NPL Oxide Database [11]). Notably, these two reactions occur at much lower oxidising atmospheres than with pure iron oxides, as seen in Fig. 1. Therefore at 1123 K, $Ca_2Fe_2O_5$ can achieve a 75% conversion of steam over the entirety of its carrying capacity of oxygen, a marked increase from 62% for unmodified iron oxide over its wüstite-iron transition (Fe_zO-Fe) or 21% for the magnetite-wüstite transition (Fe_3O_4-Fe_zO). Whilst carbonation of the reduced and oxidised forms of $Ca_2Fe_2O_5$ may occur under certain conditions, this is thermodynamically infeasible in the experimental conditions described here.

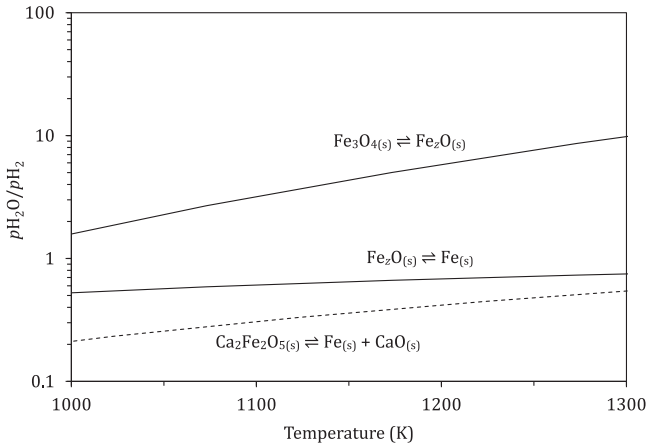

Fig. 1. Baur-Glaessner phase diagram showing the phase transitions of the Fe-O system in different oxidising environments (the steam to hydrogen ratio, pH_2O/pH_2) as a function of temperature, calculated from experimental data [7]. The phase transition for $Ca_2Fe_2O_5$-Fe + CaO (dashed) is also shown, calculated from experimental data reported by Jacob *et al.* [10].

The present work investigates the use of $Ca_2Fe_2O_5$ for the chemical looping production of hydrogen and to compare its performance against chemically unmodified iron oxide supported on ZrO_2, a system studied in an earlier work [12]. This is important in improving the efficiency of hydrogen generation *via* the steam-iron reaction.

2. Experimental

The oxygen carriers, (i) 60 wt% Fe_2O_3 supported on ZrO_2 (denoted Fe60Zr) and (ii) $Ca_2Fe_2O_5$, were synthesised using a modified Pechini method [13,14]. Briefly, stoichiometric quantities of the metal nitrates ($Fe(NO_3)_3{\cdot}9H_2O$, purity > 98%, Sigma–Aldrich; $ZrO(NO_3)_2{\cdot}xH_2O$, purity > 99.5 %, ZrO_2 content = 35.4 wt%, ACROS Organics; $Ca(NO_3)_2{\cdot}4H_2O$, purity > 99.0%, Sigma–Aldrich) were dissolved in reverse osmosis water. Citric acid (purity > 99.5%, Sigma–Aldrich) was then added with a citric acid to metal ion mole ratio of 1. Ethylene glycol (purity > 99.75%, Sigma–Aldrich) was then added to the mixture with a glycol to citric acid mole ratio of 1. The mixture was then dried at 373 K in air for 12 h to produce a xerogel, which was then calcined at 1223 K in air for 3 h. The purity of the synthesised $Ca_2Fe_2O_5$ was verified by X-ray diffraction (XRD) and thermogravimetric analysis (TGA). The oxygen carrying capacity of the samples was measured using TGA by temperature-programmed reduction in H_2 and oxidation in air. The XRD pattern and TGA data are shown in the Supplementary information. For use in a packed bed, the calcined powders were compressed at 740 MPa for 3 min followed by crushing to a sieve size range of 300–425 μm.

Details of the packed bed reactor used to examine the performance of the oxygen carriers can be found in the Supplementary information. The temperature of 1123 K was chosen to accommodate the effluent from a typical gasifier, and because carbonation is infeasible at these conditions. The oxygen carriers were reacted in sequential stages, summarised in Table 1. The durations of each stage were chosen to allow each reaction to reach completion, which was indicated by no further conversion of the inlet gases. This was intended to sample as many phase transitions as possible in the carrier. The duration of reduction of $Ca_2Fe_2O_5$ was longer

Table 1
Conditions of each stage in the experiments. Flows were measured at 295 K, 1 atm.

Stage	Inlet concentration (vol%)	Total flow rate (ml/min)	Duration (min)	
			Fe60Zr	$Ca_2Fe_2O_5$
(i) Reduction with CO	10.1	230	99	172
(ii) Oxidation with H_2O	2.5–3.5[a]	96	198	198
(iii) Oxidation with O_2	2.3	300	30	30

[a] Measured online by a capacitive relative humidity sensor (HYT 271, IST AG). Some variation arose from changes in the laboratory temperature.

because its rate of reduction with CO was strongly limited by thermodynamics. The flow rates during oxidation with steam were chosen to be sufficiently low for equilibrium to be established between H_2O, H_2 and the oxygen carrier, confirmed by a period, or periods, of constant off-gas composition. Further confirmation was indicated by the conversion of steam being unchanged when the flow rate was further decreased. The reactor was purged with N_2 for 3 min between each stage.

During oxidation with steam, the instantaneous conversion of steam at a particular time was calculated using:

$$x_{H_2O}(t) = \frac{\text{instantaneous molar flow rate of } H_2 \text{ leaving the bed}}{\text{instantaneous molar flow rate of } H_2O \text{ entering the bed}} = \frac{1}{\frac{y_{H_2O,in}}{1-y_{H_2O,in}}} \frac{y_{H_2}(t)}{1-y_{H_2}(t)} \quad (10)$$

where y_i is the mole fraction of species i in the off-gas measured on a dry basis, and $y_{H_2O,in}$ is the measured mole fraction of steam in the feed.

The cumulative conversion of steam was calculated using:

$$X_{H_2O}(t) = \frac{\text{total moles of } H_2 \text{ leaving the bed}}{\text{total moles of } H_2O \text{ entering the bed}} = \frac{1}{\frac{y_{H_2O,in}}{1-y_{H_2O,in}}} \frac{\int_{t_{start}}^{t} \frac{y_{H_2}(t)}{1-y_{H_2}(t)} dt}{t - t_{start}} \quad (11)$$

where t_{start} is the time when H_2 is first detected by the analyser.

The conversion of the bed of oxygen carrier was calculated, assuming dilute gases, using:

$$X_O(t) = \frac{\text{accumulated moles of O in reactor}}{\text{oxygen carrying capacity of sample}} = \frac{\dot{N}_{N_2}}{n_O} \int_{t_{start}}^{t} \left(\frac{y_{H_2}(t)}{1-y_{H_2}(t)} - \frac{2y_{CO_2}(t)}{1-y_{CO_2}(t)} - \frac{y_{CO}(t)}{1-y_{CO}(t)} \right) dt \quad (12)$$

where $\dot{N}_{N_2}$ is the molar flow rate of N_2 and n_O is the nominal molar oxygen carrying capacity of the carrier.

3. Results

The compositions of the off-gases from the reactor with time are shown in Fig. 2, which reflect the rate of reaction and the conversion of the bed. The lower concentration of hydrogen produced by $Ca_2Fe_2O_5$ was caused by the lower humidity of the feed due to variations in the ambient temperature affecting the saturator.

3.1. Reduction with CO

Initially, the sample was reduced with CO until negligible amounts of CO_2 were measured at the outlet (residual conversions of CO were attributed to carbon deposition by the reverse Boudouard reaction and was consistent with the evolution of carbon oxides during oxidation steps). Initially for Fe60Zr, in Fig. 2A, CO was fully converted to CO_2, corresponding to the transition of Fe_2O_3 to Fe_3O_4 with its high oxidising potential (Eq. (1)). The concentration of CO_2 then quickly dropped with time as the bed was progressively reduced and Fe_2O_3 was consumed. The point of inflection at $t = 10$ min indicated the depletion of Fe_3O_4, beyond which the majority of the reaction was due to the reduction of Fe_zO to Fe. The outlet concentration did not equilibrate with the oxygen carrier because the conversion was limited by the rate of reaction. As the lattice oxygen was depleted, the rate of reaction slowed and the conversion of CO fell.

For $Ca_2Fe_2O_5$, in Fig. 2B, an initial spike of CO_2 was observed which was probably due to contaminants in the reactor (XRD and TGA data in the Supplementary information suggested that the sample itself is pure, and control experiments in the packed bed containing only α-Al_2O_3 detected oxygen-carrying capacities of up to 3 mol% of the nominal loading). As the bed became depleted in $Ca_2Fe_2O_5$, the concentration of CO_2 dropped as the rate of reaction decreased, similar to the behaviour observed for Fe60Zr, but without an obvious point of inflection. Differences in reduction behaviour can be seen where Fe60Zr, with its higher oxidising potential, gave higher conversions of CO than $Ca_2Fe_2O_5$, and was fully reduced in a shorter time.

3.2. Oxidation with H_2O

During oxidation with steam, both materials exhibited an initial spike in H_2, probably owing to reaction with the carbon deposited during the CO reduction, indicated by the accompanying evolution of CO and CO_2. Aside from this initial removal of carbon, two distinct regimes can be observed, namely (I) equilibrium-limited and (II) rate-limited, both being marked in Fig. 2. Generally in the equilibrium-limited regime, both the chemical kinetics and mass transfer are fast enough for the reaction to be limited by the supply of the reacting gas. The conversion will then reach the thermodynamic limit at the exit from the bed. In essence, the oxides in the bed act as a redox buffer to constrain the local oxidising potential of the gas. This means that the composition profile in the equilibrium-limited regime will be constant and correspond to the oxidising potential of the material at the exit of the bed. In Fig. 2A, two plateaux can be seen in the mole fraction of H_2. The measured values of y_{H_2O}/y_{H_2} at these plateaux are 0.63 and 3.87, respectively, and are in agreement with the predicted values of 0.63 and 3.85 for the Fe_zO-Fe and Fe_3O_4-Fe_zO transitions at 1123 K, respectively. The reactor was operating in the equilibrium-limited regime at these plateaux.

For wüstite (Fe_zO), the stability of its non-stoichiometry resulted in a continuously decreasing oxidising potential as the lattice oxygen content fell at the outlet, and hence a decaying conversion of steam over time. This situation could have been confounded with the rate-limited regime, and may have been observed between the first and second plateaux for Fe60Zr, marked as II* in Fig. 2A. The rate-limited regime is associated with the depletion of lattice oxygen, leading to a gradual decrease in the rate and hence the conversion of gas. This behaviour was observed after the second plateau during the decline in y_{H_2}. For the situation in $Ca_2Fe_2O_5$, Fig. 2B, one equilibrium-limited period is initially observed followed by a rate-limited period. The observed oxidising

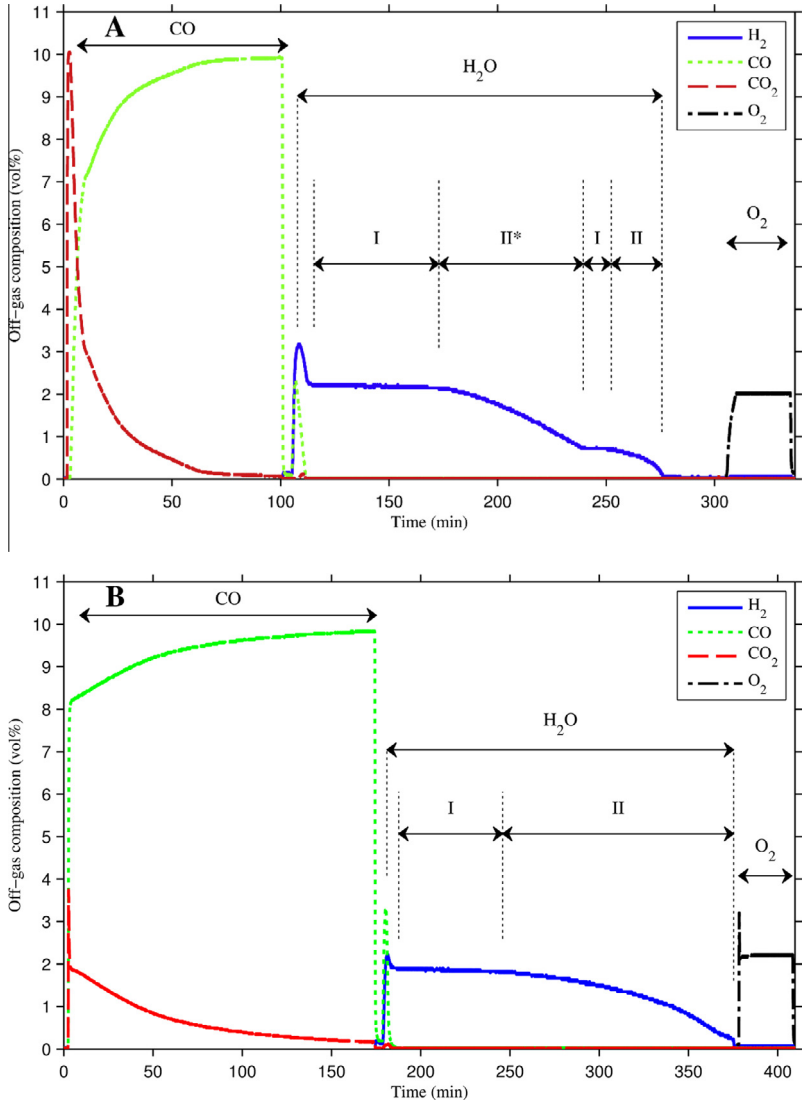

Fig. 2. Off-gas mole fraction profiles for (A) Fe60Zr and (B) $Ca_2Fe_2O_5$. Initially 10 vol% CO is fed into the bed, followed by steam and finally air. The packed bed was purged with N_2 between each step. The regimes governing the conversion of steam are labelled as I equilibrium-limited and II rate-limited. II* indicates that non-stoichiometric effects may also have been significant.

potential here was consistent with the single redox buffer described by Eq. (8) (*i.e.* its equilibrium constant).

3.3. Oxidation with air

When air was fed, the lagged breakthrough of O_2 showed that further oxidation occurred with Fe60Zr, because Fe_3O_4does not react with steam, the reverse of Eq. (4) being thermodynamically infeasible. No further oxidation was observed for $Ca_2Fe_2O_5$, which indicates that steam is sufficient to fully oxidise the material, consistent with Eq. (8) (the initial overshoot in the concentration of O_2 is an experimental artefact caused by the mixing of pressurised air and N_2). Lastly, no CO_x was evolved, indicating that the steam was sufficient to remove all carbon deposits.

The conversions of steam *versus* the conversion of the bed are shown in Fig. 3. The conversions of the bed have been normalised to reflect the difference in H_2-production capacity between unmodified iron oxide and $Ca_2Fe_2O_5$, which is 88.9% and 100% of the oxygen carrying capacity, respectively. Fig. 3 also shows ideal scenarios where the conversion of the gas was constantly equilibrium-limited, assuming that the oxidation state of the bed changed either (i) in sharp fronts propagating axially or (ii) uniformly along the bed. In ideal case ii it can be shown that, starting from the definition given in Eq. (11), the ideal cumulative conversion of steam is given by:

$$X_{H_2O,\text{ideal ii}}(X_o) = \frac{X_o}{\int_0^{X_o} \frac{1}{x_{H_2O,\text{ideal ii}}(X_o)} dX_o} \tag{13}$$

where $x_{H_2O,\text{ideal ii}}(X_o)$, the ideal instantaneous conversion of steam, is related to X_o, the conversion of the bed, from thermodynamic data [7]. It is apparent that the results match more closely the latter case, suggesting there has been considerable dispersion along the bed.

In Fig. 3 it can be seen that $Ca_2Fe_2O_5$ showed markedly higher conversions of up to 75% compared to 62% for Fe60Zr and, owing to its single phase transition, maintained a higher cumulative conversion across all states of conversion of the bed. Fe60Zr maintained 62% conversion as long as metallic iron was sufficiently active in the bed. When the metallic iron became depleted, the conversion dropped as the next least oxidising material is wüstite. The oxidising potential of wüstite is a function of its oxygen stoichiometry $1/z$ in Fe_zO [7], so as the wüstite phase was enriched

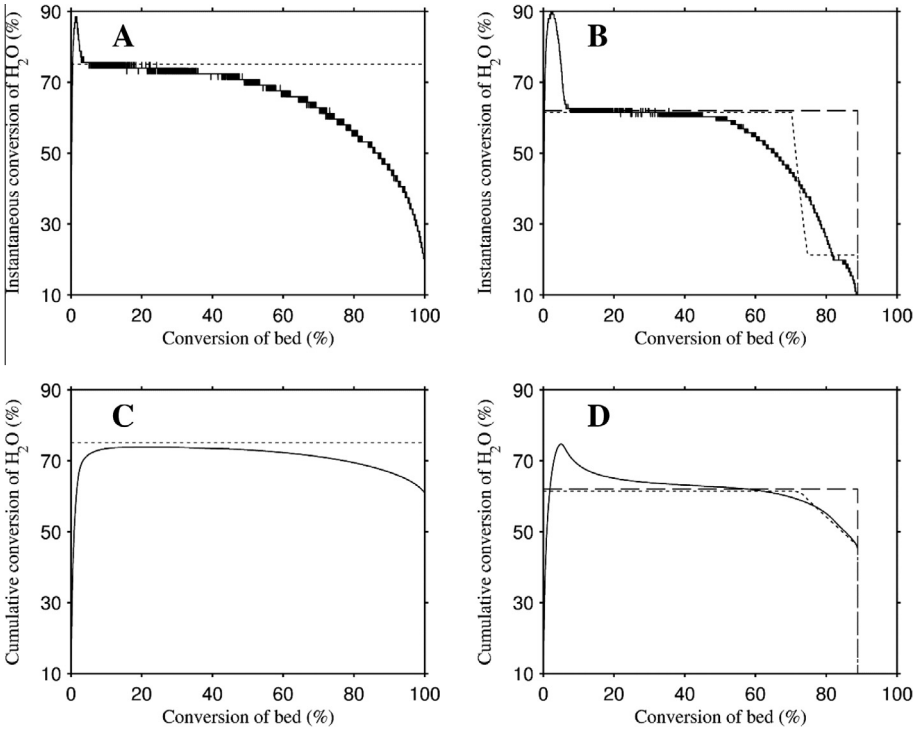

Fig. 3. Conversions of steam *versus* the conversion of the bed of oxygen carrier. (A, B) Instantaneous conversions for $Ca_2Fe_2O_5$ and Fe60Zr, respectively. (C, D) Cumulative conversions for $Ca_2Fe_2O_5$ and Fe60Zr, respectively. Solid lines, dashed lines and dotted lines correspond respectively to experimental observations, the ideal case with sharp axial fronts, and the case with a uniform distribution of oxidation states (with equilibrium being attained at all times in the last two cases).

in oxygen from $Fe_{0.950}O$, the equilibrium conversion of steam declined. The first decline in the conversion of steam was likely to be a convolution of (i) consumption of Fe and (ii) enrichment of the wüstite phase. Once wüstite became fully enriched (*i.e.* $Fe_{0.891}O$, in equilibrium with magnetite), magnetite (Fe_3O_4) started to form. This magnetite-wüstite redox buffer then maintained the conversion of steam at 21% until the wüstite was consumed, with no further hydrogen produced.

4. Discussion

The enhancement of the conversion of steam through the use of $Ca_2Fe_2O_5$ over that of chemically unmodified iron oxide has been demonstrated. Furthermore, all of the oxygen carrying capacity in $Ca_2Fe_2O_5$ was available to produce hydrogen, whereas for Fe60Zr only oxygen from oxidising Fe to Fe_3O_4 is available (which is 89 mol% of the oxygen present in Fe_2O_3). This was sustained throughout the 10 cycles tested. XRD patterns of the fresh and cycled material (in the Supplementary information) also showed that $Ca_2Fe_2O_5$ was able to be fully regenerated and did not segregate into Fe_2O_3 and CaO. In Fig. 3, the deviation of the conversion plots from ideality is due to the reactivity of the carrier decreasing as it nears full conversion. Use of longer beds or lower flow rates will be able to improve the conversion profiles, as suggested by assumptions adopted in a modelling study of fixed beds operating at equilibrium [15].

Drawbacks were observed in that $Ca_2Fe_2O_5$ gave a lower conversion of CO during reduction which could contaminate the CO_2 stream and render carbon capture and storage more difficult. Here, low conversions of CO arose from a decreased rate of reduction, but even at equilibrium at 1123 K, the maximum conversion of CO attainable by $Ca_2Fe_2O_5$ would be 23%, compared to 77% or 100% for Fe60Zr depending on if oxidation with air is used. This could be alleviated by using $Ca_2Fe_2O_5$ in a polishing operation (illustrated in Fig. 4), where the mixture of H_2 and H_2O from the outlet of a bed of unmodified iron oxide would be fed into a bed of reduced $Ca_2Fe_2O_5$. With this arrangement at 1123 K, only 17% of the H_2-production capacity (on a molar basis) needs to be provided by the $Ca_2Fe_2O_5$ stage, with the other 83% provided by the unmodified Fe stage (assuming ideal breakthrough occurs in both beds simultaneously). This requires a smaller loading of $Ca_2Fe_2O_5$ than if all of the H_2-production capacity were to be provided by $Ca_2Fe_2O_5$ alone, thus drastically decreasing the time for complete reduction whilst achieving enhanced conversions of steam.

A further improvement would be, during the reduction step, to reverse the flow of syngas so that it is first fed to $Ca_2Fe_2O_5$ and then

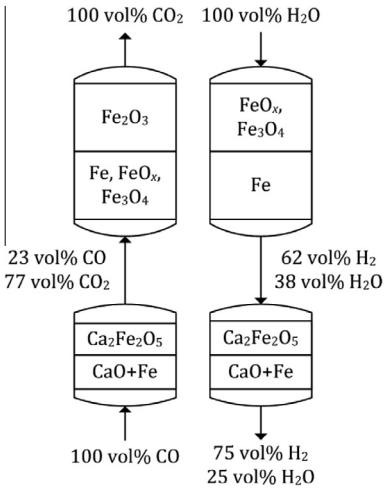

Fig. 4. Illustration of the polishing concept in combination with reversal of the flows operating at 1123 K. The flow direction during reduction (left) and oxidation (right) are reversed in order to maximise the conversion of the feed gases.

unmodified iron. Reversal of the flow maximises both the respective conversions of CO and H_2O during the reduction and oxidation steps, whereas the staged polishing arrangement decreases the amount of $Ca_2Fe_2O_5$ required for the enhancement in the conversion of steam. This configuration has also been proposed by other workers [3,9]. The reactive gases are sequentially exposed to materials of increasing driving force (*i.e.* decreasing oxidising potential for the oxidation step, or increasing oxidising potential for the reduction step).

5. Conclusions

The performance of a rationally-designed oxygen carrier $Ca_2Fe_2O_5$ was verified by comparison with 60 wt% Fe_2O_3-ZrO_2 (Fe60Zr). Experiments conducted in a packed bed reactor confirmed that, at 1123 K, $Ca_2Fe_2O_5$ achieved higher conversions of steam of 75% compared to 62% for Fe60Zr. This came at the cost of lower conversions of CO, but this can be offset with adaptations in the process design. A proposed modification is a polishing operation where the composition of the product gases (H_2 and steam) from a bed of unmodified iron oxide is polished in a subsequent bed of $Ca_2Fe_2O_5$, thus decreasing the required amount of $Ca_2Fe_2O_5$. The flow may also be reversed during oxidation and reduction, maximising the respective conversions of CO and H_2O.

Acknowledgements

Dr Matthew T. Dunstan is acknowledged for help with the XRD analysis. M.S.C.C acknowledges financial support from an EPSRC Doctoral Training Grant. W.L and Y.Y acknowledge funding from the National Research Foundation (NRF), Prime Minister's Office, Singapore under its Campus for Research Excellence and Technological Enterprise (CREATE) programme.

Appendix A. Supplementary data

Supplementary data associated with this article can be found, in the online version, at http://dx.doi.org/10.1016/j.cej.2016.03.132.

References

[1] I. Dincer, C. Acar, Review and evaluation of hydrogen production methods for better sustainability, Int. J. Hydrogen Energy 40 (2015) 11094–11111, http://dx.doi.org/10.1016/j.ijhydene.2014.12.035.
[2] P. Häussinger, R. Lohmüller, A.M. Watson, Hydrogen, 2. Production, in: Ullmann's Encycl. Ind. Chem., Wiley-VCH Verlag GmbH & Co. KGaA, Weinheim, Germany, 2000 (doi: 10.1002/14356007.o13_o03).
[3] M.V. Kathe, A. Empfield, J. Na, E. Blair, L.-S. Fan, Hydrogen production from natural gas using an iron-based chemical looping technology: thermodynamic simulations and process system analysis, Appl. Energy 165 (2016) 183–201, http://dx.doi.org/10.1016/j.apenergy.2015.11.047.
[4] A. Messerschmitt, Process of Producing Hydrogen., US971206, 1910. <http://www.google.com/patents/US971206>.
[5] C.D. Bohn, C.R. Müller, J.P. Cleeton, A.N. Hayhurst, J.F. Davidson, S.A. Scott, et al., Production of very pure hydrogen with simultaneous capture of carbon dioxide using the redox reactions of iron oxides in packed beds, Ind. Eng. Chem. Res. 47 (2008) 7623–7630, http://dx.doi.org/10.1021/ie800335j.
[6] F. He, F. Li, Hydrogen production from methane and solar energy – process evaluations and comparison studies, Int. J. Hydrogen Energy 39 (2014) 18092–18102, http://dx.doi.org/10.1016/j.ijhydene.2014.05.089.
[7] R.A. Giddings, R.S. Gordon, Review of oxygen activities and phase boundaries in wustite as determined by electromotive-force and gravimetric methods, J. Am. Ceram. Soc. 56 (1973) 111–116, http://dx.doi.org/10.1111/j.1151-2916.1973.tb15423.x.
[8] M. Ismail, W. Liu, S.A. Scott, The performance of Fe_2O_3-CaO oxygen carriers and the interaction of iron oxides with CaO during chemical looping combustion and H_2 production, Energy Proc. 63 (2014) 87–97, http://dx.doi.org/10.1016/j.egypro.2014.11.010.
[9] F. He, F. Li, Perovskite promoted iron oxide for hybrid water-splitting and syngas generation with exceptional conversion, Energy Environ. Sci. 8 (2015) 535–539, http://dx.doi.org/10.1039/C4EE03431G.
[10] K.T. Jacob, N. Dasgupta, Y. Waseda, Thermodynamic properties of the calcium ferrites $CaFe_2O_4$ and $Ca_2Fe_2O_5$, Z. Metallkd. 90 (1999) 486–490.
[11] R.H. Davies, A.T. Dinsdale, J.A. Gisby, J.A.J. Robinson, S.M. Martin, MTDATA – thermodynamic and phase equilibrium software from the national physical laboratory, Calphad 26 (2002) 229–271, http://dx.doi.org/10.1016/S0364-5916(02)00036-6.
[12] W. Liu, J.S. Dennis, S.A. Scott, The effect of addition of ZrO_2 to Fe_2O_3 for hydrogen production by chemical looping, Ind. Eng. Chem. Res. 51 (2012) 16597–16609, http://dx.doi.org/10.1021/ie302626x.
[13] M.P. Pechini, Method of Preparing Lead and Alkaline Earth Titanates and Niobates and Coating Method Using the Same to Form a Capacitor, US3330697 A, 1967. <https://www.google.com/patents/US3330697>.
[14] B.L. Cushing, V.L. Kolesnichenko, C.J. O'Connor, Recent advances in the liquid-phase syntheses of inorganic nanoparticles, Chem. Rev. 104 (2004) 3893–3946, http://dx.doi.org/10.1021/cr030027b.
[15] P. Heidebrecht, K. Sundmacher, Thermodynamic analysis of a cyclic water gas-shift reactor (CWGSR) for hydrogen production, Chem. Eng. Sci. 64 (2009) 5057–5065, http://dx.doi.org/10.1016/j.ces.2009.08.011.